Pharm Res (2013) 30:1525–1535
DOI 10.1007/s11095-013-0990-y

RESEARCH PAPER

Characterization of Spherulites as a Lipidic Carrier for Low and High Molecular Weight Agents

Peng Zhang • Yixian Huang • Alexander M. Makhov • Xiang Gao • Peijun Zhang • Song Li

Received: 16 November 2012 / Accepted: 22 January 2013 / Published online: 12 April 2013

ABSTRACT

Purpose To develop spherulite formulations to achieve high entrapment efficiency for both small and macromolecules as well as cell-type specific delivery.

Methods Spherulites of various compositions were prepared, and lipid-PEG was incorporated through post-insertion. Calcein and FITC-labeled albumin were employed as model drugs for small and macromolecules. The spherulites were characterized with respect to entrapment efficiency, size, structure, and release kinetics, and the morphology was examined *via* cryo-EM. Finally, SV119-decorated spherulites were examined for their selective uptake by cancer cells.

Results The spherulites are 170 ~ 290 nm in size. A loading efficiency of 55 ~ 60% can be consistently achieved for both calcein and albumin under optimized conditions. Cryo-EM shows the onion-like morphology consistent with the structure of multilamellar liposomes. A $t_{1/2}$ of 39.3 h and 69.7 h in cargo release in serum was observed before and after PEG decoration, and incorporation of SV119 led to selective delivery of rhodamine-labeled spherulites to PC-3 tumor cells.

Conclusions Our optimized formulations may represent a platform with simple preparation approach, relatively small particle size, high drug loading efficiency for both low and high molecular weight agents, and slow release kinetics for selective delivery of various types of therapeutics to target cells.

KEY WORDS cryo-electron microscopy · entrapment efficiency · multilamellar liposomes · spherulites · targeted drug delivery

ABBREVIATIONS

BS10	brij S10
BSA	bovine serum albumin
CH	cholesterol
Cryo-EM	cryo-electron microscopy
Dex	dexamethasone
DLS	dynamic light scattering
DMEM	Dulbecco's modified eagle's medium
DPBS	Dulbecco's phosphate buffered saline
$DSPE\text{-}PEG_{2k}$	1,2-distearoyl-sn-glycero-3-phosphoethanolamine-N-[amino(polyethylene glycol)-2000]
EE	entrapment efficiency
EPR	enhanced permeability and retention
FBS	fetal bovine serum
FITC	fluorescein isothiocyanate
FITC-BSA-SU	fluorescein isothiocyanate-labeled succinylated bovine serum album
$MeO\text{-}PEG_{5k}$	methoxypoly(ethylene glycol)-5000
MLV	multilamellar vesicles
SPC	soybean L-α-phosphatidylcholine
TW80	polyoxyethylene 80 sorbitan monooleate

P. Zhang • Y. Huang • X. Gao • S. Li (✉)
Center for Pharmacogenetics, Department of Pharmaceutical Sciences
School of Pharmacy, University of Pittsburgh, 639 Salk Hall
Pittsburgh, Pennsylvania 15261, USA
e-mail: sol4@pitt.edu

A. M. Makhov • P. Zhang
Department of Structural Biology, School of Medicine
University of Pittsburgh, Pittsburgh, Pennsylvania 15261, USA

INTRODUCTION

There are several major barriers in drug development such as poor water solubility of the drug candidates, short circulating time *in vivo* due to rapid elimination and clearance, and lack of selectivity towards target tissue(s). In addition, macromolecule-based therapeutics may suffer from poor stability *in vivo* due to the hydrolytic activities of proteases

and nucleases present in biological fluids. Formulation development represents an important strategy to overcome these problems (1–6).

Liposomes have long been studied as a carrier for various types of therapeutic agents and several liposomal drugs are currently used in the clinic for the treatment of cancers and infectious diseases (7–10). There are a number of advantages with liposomal systems compared to other delivery systems such as excellent biocompatibility and biodegradability, and the capability of loading both hydrophilic and hydrophobic drugs. Passive-targeting of liposomal drugs to tissues with leaky vasculature (*e.g.*, tumors) can also be achieved through the enhanced permeability and retention (EPR) effect based on the nano scale size of the vesicles (11, 12). Finally, active-targeting can be achieved *via* surface decoration with a ligand specific for a receptor that is over-expressed on the target cells (13, 14).

Most of the studies with liposomal systems involve the use of unilamellar liposomes (8–10) due to the well-controlled size. However, except for few compounds with weak amines or acids that can be quantitatively encapsulated inside liposomes *via* remote loading method (15), unilamellar liposomes suffer from a low drug-loading capacity for most therapeutic agents. This is particularly the case for loading of macromolecules (*e.g.*, proteins, DNA etc.) with neutral or anionic unilamellar liposomes.

Unlike unilamellar liposomes, multilamellar liposomes (MLV) have much improved drug loading capacity, particularly for macromolecules. MLV are often prepared *via* solvent evaporation method. This method has the drawbacks of exposing the drugs to organic solvents, relatively large sizes and heterogeneous size distribution. These problems, however, are not shared by spherulites, a different type of MLV (16–19). These liposomes were prepared *via* hydrating dried lipid films with a minimal volume of aqueous solution, followed by shearing of the hydrated lipids with low mechanical force. Spherulites are unique onion-like structures composed of multiple concentric phospholipid bilayers alternating with layers of aqueous medium and typically small aqueous inner cores. Both small and macromolecules can be loaded into spherulites with high efficiency. Another advantage for the spherulite formulation is the minimal risk of denaturation of macromolecule cargos due to the low-shearing force applied during encapsulation. Preparation of spherulites also avoids exposure of cargos to organic solvent, which further minimizes the damage to the protein cargos. Finally, the unique multi-layer structure may provide a slow-release mechanism that may be useful for achieving prolonged drug action. Since the 1st report of their application as a drug carrier by Roux and colleagues in 1993, spherulites have been employed for quantitative encapsulation of both small and macromolecules including proteins and oligodeoxynucleotides (ODNs) (20).

The biophysical property of drug-loaded spherulites is affected by many factors such as lipid composition, shear force, and the type of cargos to be loaded *etc*. However, much more remains to be understood about the factors contributing to an optimal spherulite preparation for small and macromolecules. In addition, it is unknown if targeted delivery of spherulites to tumor cells can be achieved *via* surface decoration with a small molecule ligand. In this study, systematic studies were conducted to examine how the lipid composition affects the loading efficiency, size, and the release kinetics using fluorescence and albumin as model small and macromolecules. The morphology of the spherulites was examined *via* cryo-EM. Finally, a small molecule ligand for σ-2 receptor (SV-119) was incorporated into spherulites and the selective uptake of ligand-decorated spherulites was examined in human prostate cancer cells that overexpress σ-2 receptor.

MATERIALS AND METHODS

Materials

L-α-phosphatidylcholine (Soy-95%) (SPC), rhodamine PE, and 1,2-distearoyl-sn-glycero-3-phosphoethanolamine-N-[amino(polyethyleneglycol)-2000] (DSPE-PEG_{2k}) were purchased from Avanti Polar Lipids Inc. (Alabaster, AL, USA). Brij S10 (BS10), polyoxyethylene 80 sorbitan monooleate (TW80), cholesterol (CH), dexamethasone (Dex), methoxypoly(ethylene glycol)-5000 (MeO-PEG_{5k}), bovine serum albumin (BSA), fluorescein isothiocyanate (FITC), calcein, and Triton X-100 were obtained from Sigma-Aldrich (St. Louis, MO, USA). Sepharose 4B, Sephadex G-25 and Sephacryl S-100 were obtained from GE Healthcare (Piscataway, NJ). Dulbecco's phosphate buffered saline (DPBS), Dulbecco's modified eagle's medium (DMEM), and opti-MEM reduced serum medium were all purchased from Gibco Life Technologies (Carlsbad, CA). Fetal bovine serum (FBS) was obtained from Invitrogen (Carlsbad, CA). All other chemicals and organic solvents were purchased from Sigma-Aldrich without further purification. Water was deionized with a Barnstead Nanopure Infinity Ultrapure Water System from Thermo Scientific (Dubuque, IA, USA). ^{1}H NMR spectra were recorded on a Bruker FT 400 MHz.

Preparation of Empty Spherulites

The spherulites were prepared according to Diat et al. (17). Briefly, SPC, TW80 (or BS10) (in ethanol at 0.5 g/ml) and CH (in chloroform at 0.1 g/ml) were mixed at various molar ratios. The solvent was evaporated by a steady flow of nitrogen gas. A trace amount of organic solvent was removed *via* vacuum at room temperature for 2 h. The dried lipids were hydrated with 10 mM pH 7.0 Tris–HCl buffer at a weight

ratio of 1:1 to total lipids at room temperature overnight. The hydrated lipids were then gently sheared for 5 min manually using a plastic paddle that is well-matched with the tube, followed by dilution with buffer to suspend the formed vesicles. The procedure for the preparation of spherulites was illustrated in Fig. 1.

Preparation of FITC-Labeled Succinylated BSA (FITC-BSA-SU)

Calcein and albumin were used as water soluble small and macromolecular model drugs, respectively. In order to follow albumin entrapment, BSA was conjugated with a fluorescence marker, FITC. In addition, BSA was succinylated to reduce the potential destabilization effect of free amino groups on lipid membrane. Briefly, FITC (4-fold molar excess) in DMSO was added dropwise to BSA in 0.5 mol/l potassium bicarbonate under stirring. The reaction was kept in dark for 2 h. Two ml of the reaction mixture was then dialyzed against 4 changes of 500 ml of water through a dialysis tubing (33 mm×100 mm, MWCO 12,000– 14,000, Fisher Scientific Inc., USA) for 2 d at 4°C in dark, followed by lyophilization to obtain the orange powder of FITC-BSA. For succinylation, FITC-BSA was dissolved in 0.5 mol/l potassium bicarbonate and succinic anhydride in DMSO (20-fold molar excess) was added dropwise. The reaction was allowed for 2 h in dark, during which the pH was carefully controlled around 8–9. Two ml of the reaction mixture was then dialyzed against 4 changes of 500 ml of water through a dialysis tubing (33 mm×100 mm, MWCO 12,000– 14,000) for 2 d at 4°C in dark, followed by lyophilization to obtain the powder of FITC-labeled succinylated BSA (FITC-BSA-SU).

Encapsulation of Cargo Drugs and Determination of Entrapment Efficiency

Calcein-loaded spherulites were similarly prepared as described above except that calcein (50 mM) in 10 mM Tris–HCl buffer (pH 7.0) was used. The free unencapsulated calcein was removed by size-exclusion chromatography on a Sephacryl S-100 column equilibrated with Tris–HCl buffer. Protein-loaded spherulites were prepared by hydration with a 10 mM pH 7.0 Tris–HCl buffer containing FTIC-BSA-SU at 200 mg/ml, and purified through a Sepharose 4B column. The amount of calcein or protein entrapped in the spherulites was determined by measuring fluorescence intensity at 495 nm (excitation) and 521 nm (emission) on a Wallac Victor 1420 Multilabel Counter (Perkin Elmer Inc., Waltham, MA, USA) after lysing the spherulites with 0.1% (v/v) Triton X-100. The drug encapsulation efficiency was calculated by: EE% = weight of encapsulated cargo/weight of input cargo × 100%

Synthesis of MeO-PEG$_{5k}$-DOA Conjugate

The procedure for synthesizing MeO-PEG$_{5k}$-DOA conjugate is depicted in Scheme 1. The compound **2** (DOA, dioleyl amido aspartic acid) was synthesized and chemically characterized following our published method (21). Briefly, a mixture of Boc-aspartic acid (1 equiv.), oleyl amine (3 equiv.), DCC (3 equiv.), and DMAP (0.1 equiv.) were dissolved in anhydrous CH_2Cl_2 and stirred for 5 h at room temperature. After removing the solvent, the Boc-dioleyl amido aspartic acid was purified by flash column chromatography (MeOH: $CHCl_3$ 1:9) which was then stirred in trifluoroacetic acid/CH_2Cl_2 solution (1:1, v/v) for 2 h to remove the Boc moiety. The residue was purified by flash column chromatography (MeOH:$CHCl_3$ 1:9) to afford the product (compound **2**). Compound **3** was obtained *via* reacting MeO-PEG$_{5k}$-OH (1 eqiv.), succinic anhydride (5 eqiv.) and DMAP (5 eqiv.) in $CHCl_3$ following a reported procedure (22).

A solution of compound **3** (5 g, 1 mmol) in CH_2Cl_2 (5 ml) was treated with DCC (0.41 g, 2 mmol), DMAP (0.12 g, 1 mmol), and compound **2** (DOA) (689 mg, 1 mmol). The reaction vessel was capped and stirred overnight. After the reaction was completed, 100 ml Et_2O was added and the mixture was filtered to afford the crude product**.** The crude

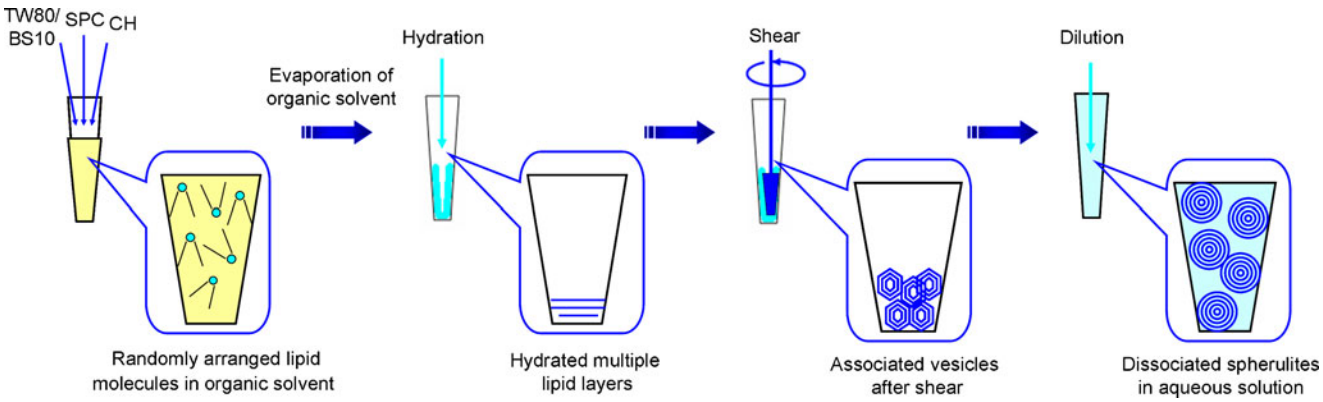

Fig. 1 Preparation approach of the spherulites through shearing method.

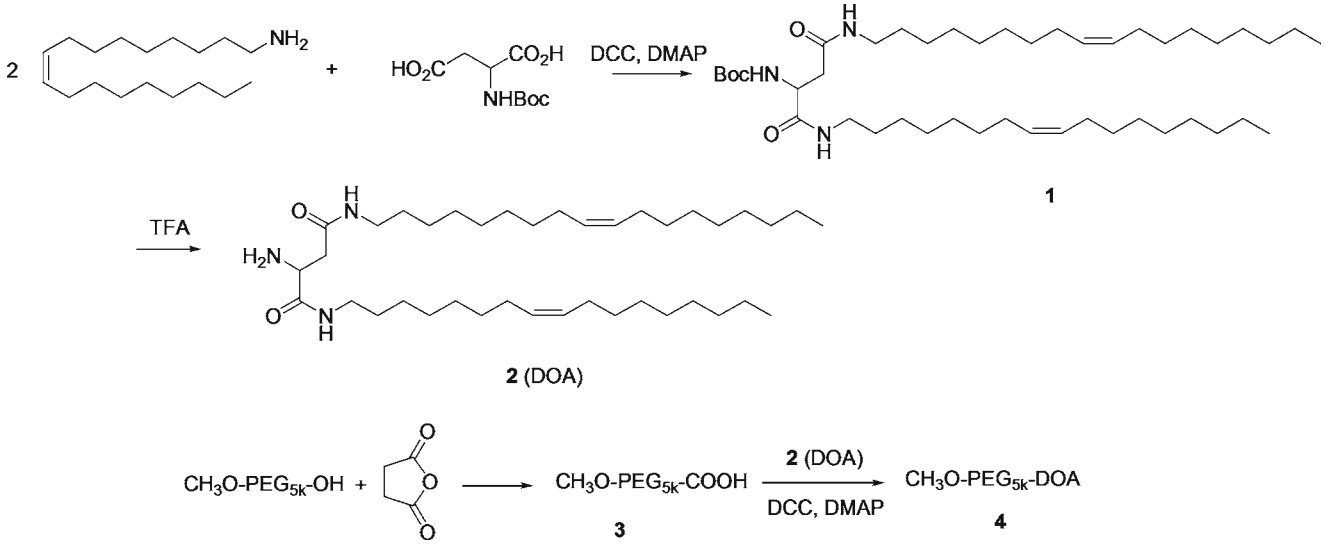

Scheme 1 Synthetic route for MeO-PEG_{5k}-DOA

product was purified by flash chromatography with silica gel (MeOH: CH_2Cl_2, 1:10) and pure MeO-PEG_{5k}-DOA (4) was obtained as a white solid with a yield of 70% (2.1 g). ^{1}H NMR ($CDCl_3$) δ5.25 (m, 4H), 3.38 (s, 3H), 3.21 (m, 4H), 2.47–2.66 (m, 6H), 2.00 (m, 4H), 1.98 (m, 7H), 1.20–1.40 (m, 48H), 0.88 (t, 6H).

Synthesis of SV119-$PEG_{3.5k}$-DOA Conjugate

The structure of SV119-$PEG_{3.5k}$-DOA conjugate is shown in Fig. 2. The synthesis and chemical characterization of SV119-$PEG_{3.5k}$-DOA was performed following our published method (21).

Surface Modification of Spherulites with PEG-DOA

A post-incorporation approach was used for PEG surface decoration of spherulites (23). Briefly, spherulites were prepared as described above. In a separate vial, MeO-PEG_{5k}-DOA micelle (0.3 μM) was prepared *via* solvent evaporation followed by hydration in Tris–HCl buffer. MeO-PEG_{5k}-DOA micelles (3 mol%) were then mixed with the preformed spherulites and the mixture was incubated at 60°C for 1 h, followed by gel filtration on a Sepharose 4B column (1.5 × 20 cm) to remove any non-incorporated PEG.

Particle Size Analysis

The spherulites were diluted to approximately 0.2 mg/ml in 10 mM pH 7.0 Tris–HCl buffer. The mean diameter of the spherulites was measured by dynamic light scattering (DLS) at 90° angle using a Coulter N4Plus (Coulter Electronics, Miami, FL). All of the measurements were performed in triplicate at 25°C.

Cryo-Electron Microscopy (Cryo-EM)

The solution (3.5 μl) of spherulites in 10 mM Tris–HCl, pH 7.0 buffer without dilution or diluted five times in water was applied onto R 2/1 Quantifoil holey carbon EM grids (Quantifoil Micro Tools GmbH, Jena, Germany). The grids containing the samples were then mounted onto an FEI Vitrobot MARK III (FEI Corp., OR.), blotted for 3–4 sec at 100% humidity, and plunge-frozen in liquid ethane. The frozen grids were loaded onto a Gatan 626 single tilt liquid nitrogen cryo holder (Gatan, Inc., Warrendale, PA, USA)

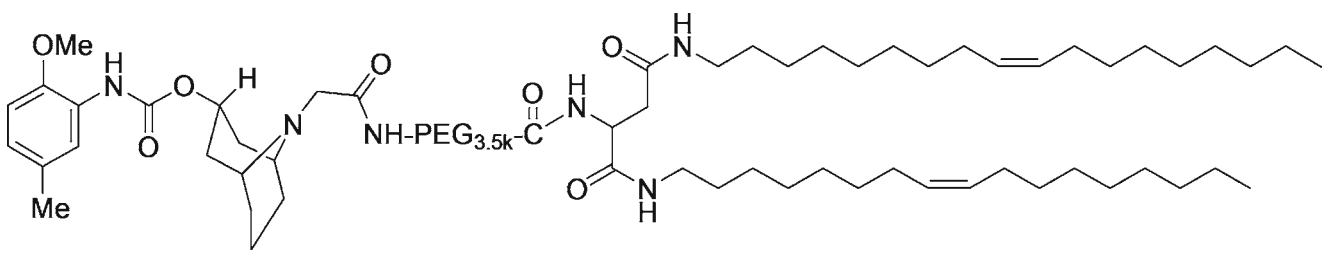

Fig. 2 Structure of SV119-$PEG_{3.5k}$-DOA.

and imaged at 200 kV with an FEI TF20 microscope (FEI Corp., OR.). Low-dose projection images were recorded on a 4 k × 4 k UltraScan 4000 CCD camera (Gatan, Inc., Warrendale, PA, USA) at under focus of 1–1.5 μm and nominal magnifications of 10,000x-50,000x. The measurements were done using the Gatan Digital Micrograph software.

In Vitro Drug Release

Fluorescence dye calcein was encapsulated into spherulites, and calcein-loaded spherulites were purified as described above. The spherulites (3 mg lipids/ml) were incubated in 10 mM pH 7.0 Tris–HCl buffer with or without 50% (v/v) FBS at 37°C, and the fluorescence intensities were measured at 0, 24, 48 and 72 h at 495 nm (excitation) and 521 nm (emission). The total fluorescence release (Ft) was determined by measuring the fluorescence intensity following the lysis of spherulites by 0.2% Triton X-100. The release of calcein was determined as follows:% Release = $(Fx–F_0)/(Ft–F_0)\times100\%$, in which F_0 and F_x are the fluorescence intensity at the beginning and at predefined time points.

Uptake of SV-119-Decorated, Rhodamine PE-Labeled Spherulites by PC-3 Cells

Human prostate cancer PC-3 cell line was obtained from American Type Culture Collection (Rockville, MD), and cultured as a monolayer in DMEM medium supplemented with 10% FBS and 1% penicillin-streptomycin at 37°C in a humidified atmosphere containing 5% CO_2. σ-2 receptor-targeted spherulites were prepared *via* postinsertion method with 3 mol% of SV119-$PEG_{3.5k}$-DOA and they share a similar lipid composition as that of formulation **5**. Controls include spherulites with 3 mol% of MeO-PEG_{5k}-DOA, 3 mol% of PEG_{2k}-DSPE, or no PEG decoration. All formulations contain 0.2 mol% of rhodamine-PE to label the spherulites. For uptake study, PC-3 cells grown in a monolayer were washed three times by DPBS, and incubated with spherulites diluted in Opti-MEM media at 37°C with a final lipid concentration of 0.9 mg/ml. Two hours following the incubation, the cells were washed three times with DPBS to remove unbound spherulites. The cell-associated fluorescence was examined under a Nikon Eclipse TE300 Inverted Fluorescent Microscope (Nikon Metrology, Inc., Brighton, MI, USA).

RESULTS AND DISCUSSION

Preparation and Characterization of Spherulites

It has been long known that, when hydrated lipid films are agitated or disturbed by an external force, the lipids layers have the tendency to detach to form self-closed vesicles in order to minimize the exposure of hydrophobic tails of the lipids to water molecules. The vesicles obtained usually have a large aqueous compartment surrounded by multilamellar bilayer membrane structures with relatively large particle size, and are heterogeneous in size distribution. Typically these MLVs are then down-sized to obtain unilamellar lipid vesicles using processes that involve stronger energy input such as sonication and extrusion (24). The entrapment efficiency is typically low due to the fact that vesicles have to go through multiple cycles of breakdown and resealing processes during which most of the initial entrapped content is lost. Some efforts have been made to improve the drug loading capacity for MLV, particularly for macromolecules such as proteins. For example, reverse phase evaporation method has been developed to encapsulate protein and DNA into MLV.

Spherulites are a different type of multilamellar liposomes that are generated *via* moderate shearing on fully hydrated lipid sheets (17–19). This protocol has several advantages over solvent evaporation method including high entrapment efficiency, and relatively mild operation procedure that does not denature proteins that are sensitive to organic solvents, excessive temperature or shear force. In this study we characterized several spherulite formulations *via* examining the effect of formulation composition on the size, loading capacity, and the release kinetics of calcein- and albumin-loaded spherulites. Furthermore, we examined if spherulites can be decorated with a small molecule ligand to achieve cell-type-specific delivery.

We initially examined the effect of lipid composition on the size of empty spherulites. Spherulites were prepared *via* hydration of the lipid films with minimal amount of aqueous solution followed by moderate shearing of the hydrated lipids using a "home-made" plastic paddle that was well matched with the tubes. Figure 1 illustrates the protocols for the preparation of spherulites. Table 1 shows the sizes of spherulites of various lipid compositions, which were all below 300 nm in diameter. For BS10-containing spherulites (formulation **4–6**), the sizes were around 260–290 nm. TW80-containing spherulites (formulation **1–3**) had substantially smaller sizes (170–200 nm in diameter), suggesting that the structure of surfactants has a significant effect in controlling the sizes of the spherulites. This is consistent with the study by Simard *et al.*, in which they showed that Tween 20 and 80 provided spherulites with smaller sizes than another surfactant, Solutol HS 15 (25). The underlying mechanism for the reduced size of TW80 formulations is likely due to its relatively high HLB value and small packing parameter based on its relatively large hydrophilic head group. The relatively large head group of TW80 can better accommodate the void created in SPC bilayers with high curvature, especially in the inner bilayers. The importance

Table 1 Formulation Composition, Particle Sizes and Entrapment Efficiency of the Spherulites

Formulation (m/m)		Empty	Calcein-loaded spherulite		Albumin-loaded spherulite	
		Particle size (nm)	Particle size (nm)	EE (%)	Particle size (nm)	EE (%)
#	SPC/TW80/CH					
1	58/13/29	174.67±16.47	165.60±6.91	30.64±2.25	168.43±6.62	45.74±2.68
2	68/15/17	203.47±13.49	180.53±6.05	29.02±3.04	148.53±12.06	42.60±4.45
3	82/18/0	170.10±4.75	165.73±9.58	12.97±1.56	156.05±18.35	29.52±0.78
	SPC/BS10/CH					
4	57/14/29	289.57±8.08	275.00±8.54	54.96±3.52	258.10±23.89	60.59±5.44
5	67/17/16	267.87±14.75	267.37±11.09	47.88±2.08	268.40±4.86	55.29±3.54
6	80/20/0	287.63±2.14	271.20±20.50	44.34±1.19	259.70±3.60	54.47±2.51
	SPC/CH					
7	80/20	526.95±109.75				

of surfactant was further demonstrated by the extremely large particle size when surfactant was removed (formulation **7**, Table 1). In contrast, when the mol% of surfactant is fixed, changes in the amounts of cholesterol only had a mild effect on particle sizes (Table 3).

After examining the effect of lipid composition on the size of empty spherulites, we went on to study how it affects the loading of both small-(calcein) and large-(BSA) sized molecules into spherulites. Similar to the effect on cargo-free spherulites, the inclusion of TW80 led to significant reduction in the size of cargo-loaded spherulites (Table 1). However, TW80-containing spherulites (formulations **1–3)** also had a lower entrapment efficiency (EE) for both calcein (13%–31%) and protein (29%–45%), compared with BS10-containing formulations (formulations **4–6)**, in which an EE of 55% and 61% was routinely achieved for calcein and albumin, respectively (Table 1). Our data showed that the choice of surfactant also has a significant impact on the EE of the vesicles. It should be noted that, although TW80 and BS10 have a carbon chain of same length (C18), TW80 has a double bond at C9-C10 position, which makes the lipid bilayers more fluidic at room temperature. In contrast, BS10 has a saturated chain with a higher melting temperature, which renders the lipid membrane stiffer and less permeable to the cargos. In addition, the different hydrophilic head groups of TW80 and BS10 can lead to different degree of hydration and different affinity between lipid membrane and the hydrophilic cargos, which also contribute to the difference in the entrapment efficiency.

Compared with formulation **3,** which does not contain CH, TW80-containing formulations (1, 2) with increased contents of CH clearly showed an improved EE for both calcein and protein, suggesting a role of cholesterol in enhancing the EE for the spherulites. For BS-10 containing formulations **4–6**, a similar trend was observed, but to a lesser extent. Cholesterol is known to increase the packing order in lipid bilayers, which leads to decreased lipid fluidity and membrane permeability (26–28). The tightly packed lipid bilayers effectively prevent the leakage of the entrapped cargos, resulting in an enhanced EE.

Table 2 shows that increases in the concentrations of input cargo used in the hydration step had little effect on the particle size and EE, but resulted in significant increases in the absolute amounts of cargos loaded into these vesicles. Increasing the BSA concentration from 50 to 200 mg/ml led to a 7-fold increase in the final protein/lipid ratio for formulation **4**.

The structure of spherulites revealed by Cryo-EM showed onion-like concentric multilamellar lipid bilayers with a minimal inner aqueous compartment (Fig. 3a). Lipid layers alternate with aqueous layers with an average spacing of 4.7 ± 1.1 nm (n=89). The sizes of spherulites under cryo-EM were somewhat smaller than those measured by DLS, probably because larger spherulites are preferentially blotted away

Table 2 Impact of Cargo Concentration on Particle Sizes, Entrapment Efficiency, and Drug/Carrier Ratios of Spherulites

Formulation #	Albumin concentration (mg/ml)	EE (%)	Albumin/lipids ratio (w/w)	Particle size (nm)
4	200	60.59±5.44	0.112±0.010	258.10±23.89
	100	49.91±2.51	0.046±0.002	244.20±18.92
	50	51.16±1.70	0.024±0.001	254.65±23.65

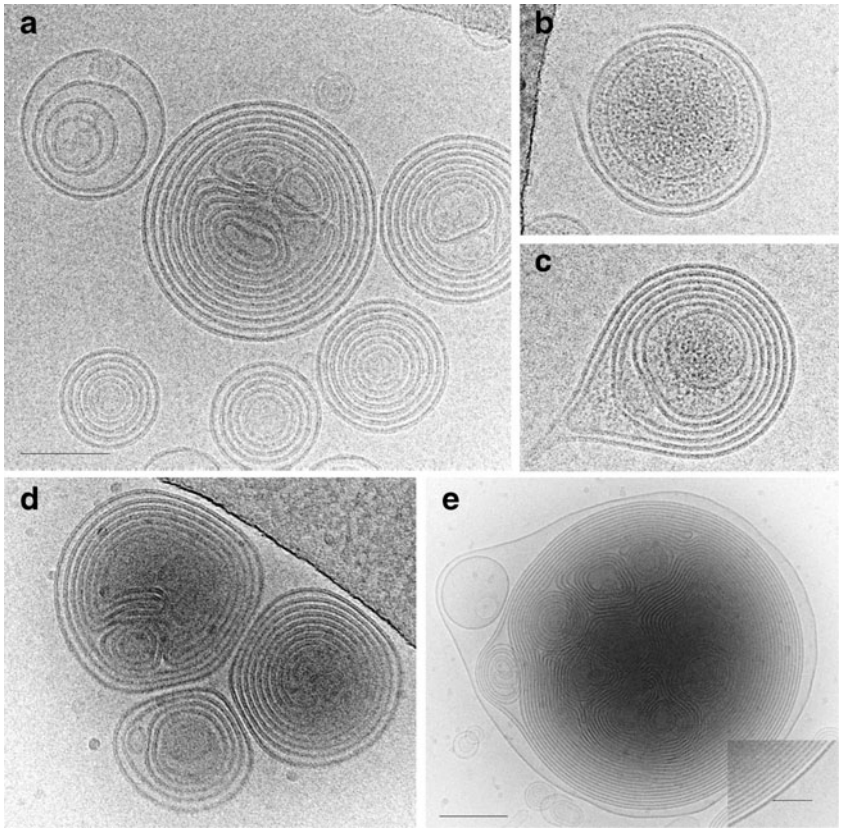

Fig. 3 Cryo-EM images of empty spherulites (**a**), BSA-loaded spherulites (**b**, **c**), and PEGylated spherulites (**d**, **e**). Image in E was recorded at lower magnification to enclose a large spherulite. Inset in E is an enlarged area of a PEGylated spherulite at the outmost lipid layer, showing dense outer lipid layer (*arrow*). All panels are in the same scale, except panel E. Scale bards, 100 nm in A and 200 nm in E.

during cryo-EM sample preparation. While empty spherulites showed low electron density between lipid layers, the spherulites loaded with BSA clearly displayed substances with increased density entrapped within vesicles (Fig. 3b, c), suggesting an efficient encapsulation of protein macromolecules.

Cargo Release Kinetics of Spherulite *In Vitro*

Release kinetics of encapsulated cargos from spherulites was evaluated at 37°C first in Tris–HCl pH 7.0 buffer and then in the presence of 50% serum to mimic the *in vivo* physiological conditions. A simple and sensitive calcein fluorescence dequenching assay was used (29). The percentage of calcein released over time was depicted in Fig. 4. It is obvious that TW80-containing formulation **1** had a much faster release kinetics in both Tris–HCl buffer (Fig. 4a) and serum (Fig. 4b) than the BS10-containing formulation **4,** which had a half-life of 39.3 h and longer than 72 h in serum and buffer respectively. Formulation **6**, which does not have CH but has the same SPC/BS10 ratio as formulation **4**, also showed a much faster release kinetics than formulation **4**. These data were consistent with the data of entrapment efficiency, suggesting again an important role of cholesterol and the surfactant structure in improving the stability of spherulites. Previously, a $t_{1/2}$ of ~8 h was reported for calcein-loaded unilamellar liposomes composed of SPC and CH (30). The much slower release kinetics of spherulites over unilamellar liposomes is likely related to the multilayer structure that allows prolonged release of loaded cargos from each enclosed compartments. Therefore, spherulites may serve as a slow-release system to achieve sustained biological effect. More studies are needed to better address this issue.

The Effect of PEGylation on Cargo Release Kinetics

It has been previously shown that liposomes interact with serum components that causes lipid exchange and membrane fusion, which leads to lipid membrane destabilization and leakage of the encapsulated cargos. Furthermore, several classes of serum proteins, named opsonins, can coat liposome surface, and "opsonized" liposomes can be recognized and rapidly taken up by phagocytes in the liver and spleen (31, 32). Decoration of nanoparticle surface with a flexible hydrophilic PEG layer has been widely used to inhibit the binding of opsonins and minimize the clearance by phagocytes (33–35). To examine if the stability of spherulites can be further improved *via* PEGylation, MeO-PEG_{5k}-DOA, a lipid-PEG conjugate, was incorporated onto the surface of the spherulites by post-insertion approach and the release kinetics of PEG-modified spherulites was compared to that of unmodified spherulites. DOA (dioleyl amido aspartic acid) is a synthetic double-chain lipid derived from aspartic acid and two carbon chains of oleylamine. Following conjugation to PEG of

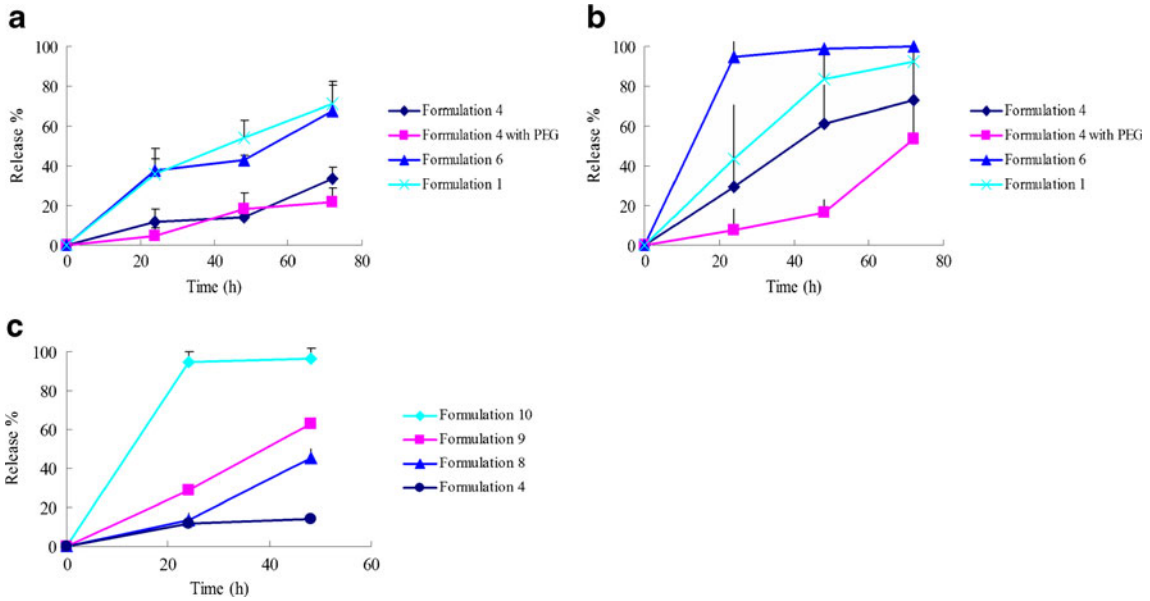

Fig. 4 Cargo release kinetics at 37°C in Tris–HCl buffer (**a**, **c**), and 50% FBS (**b**).

5000 Da, DOA can facilitate the insertion of PEG-lipid conjugate into the lipid membrane of the spherulites. DOA-PEG is a charge-neutral conjugate that can be made from readily available starting materials at low costs. The added succinyl spacer may potentially render the PEG-DOA conjugate more biodegradable than the PEG-PE derivatives. PEG-DOA micelles were incubated with pre-formed spherulites as described in (23), to ensure that the conjugate is primarily inserted onto the outer layers of the multilamellar vesicles. PEGylation by this method, as opposed to direct addition to the lipid mixture before hydration is less wasteful, and also avoids the possible destabilization effect of spherulites by these conjugates. As shown in the cryo-EM images (Fig. 3d, e), PEGylated spherulites showed a similar morphology with a similar spacing of 4.9 ± 1.1 nm (n=109) between the layers (Fig. 3d), compared to those without PEG-lipid conjugates (Fig. 3a). Interestingly, some large PEGylated vesicles (> 1 μm in diameter) display a dense and thicker outer lipid layer (Fig. 3e and inset), which is absent in non-PEGylated spherulites. Since PEG was incorporated into pre-formed spherulites, the dense outer layer most likely corresponds to additional PEG density decorating the outmost lipid layer.

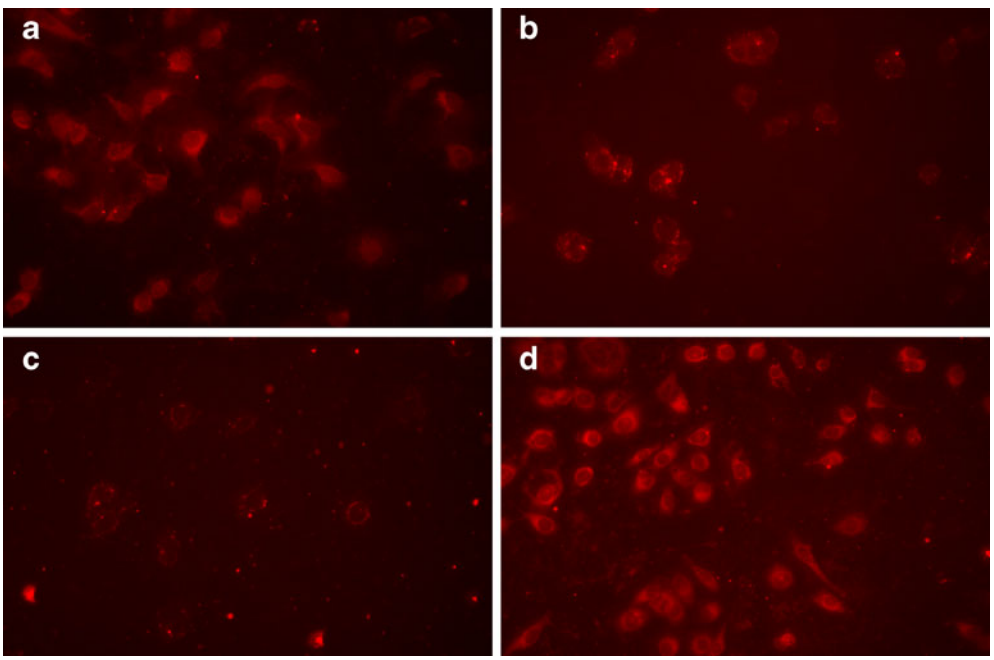

Fig. 5 Cellular uptake of rhodamine-PE labeled non-decorated (**a**), PEG_{2k}-DSPE (**b**), PEG_{5k}-DOA (**c**), and SV119-$PEG_{3.5k}$-DOA (**d**) decorated spherulites in PC-3 cell line at 37°C for 2 h.

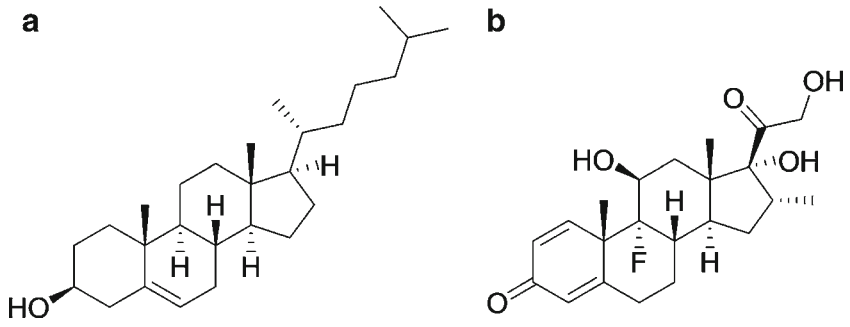

Fig. 6 Chemical structure of cholesterol (**a**) and dexamethasone (**b**).

PEGylation had minimal effect on the kinetics of calcein release for formulation **4** in Tris–HCl buffer (Fig. 4a). This may be due to the already relatively excellent stability of this formulation in the absence of serum within the short period of observation: only a low level of calcein was shown for formulation **4** in Tris buffer. As expected, exposure of the formulation to serum (50%) led to accelerated release of calcein, suggesting that serum induced destabilization of the spherulites (Fig. 3b). However, such serum effect on formulation **4** was significantly inhibited by PEGylation. PEGylated spherulites were able to maintain a slow release kinetics with a $t_{1/2}$ of 69.7 h, which is compared favorably to non-PEGylated spherulites ($t_{1/2}$, 39.3 h).

SV-119-Mediated Selective Cellular Uptake of Spherulite in PC-3 Prostate Cancer Cells

Our studies demonstrate spherulites as a carrier with improved encapsulation efficiency and stability for both small and macromolecules. To explore the possibility of ligand-guided cell type-specific delivery of spherulites, SV119, a σ-2 receptor ligand, was selected as a model ligand to enhance the selective uptake of the vesicles by tumor cells. Recently, σ-2 receptor has attracted increasing attention in tumor imaging and targeted therapy due to its overexpression in various types of human tumors such as prostate cancer, breast cancer and melanoma (36, 37). In addition, a correlation has been demonstrated between the expression level and tumor proliferation state *in vitro* and *in vivo* (38, 39). SV-119 has been used by us and others for selective delivery of various types of therapeutics to cancer cells (21, 40–42). In this study, SV119 was coupled to a lipid (DOA) through a spacer of $PEG_{3.5k}$. SV119-$PEG_{3.5k}$-DOA was synthesized following our published method (21), and incorporated onto the outer layers of the spherulites *via* post-insertion approach. Cellular uptake of SV-119-targeted spherulites by PC-3 prostate cancer cells was examined with rhodamine-PE-labeled spherulites.

Unmodified spherulites had an extensive non-specific interaction with PC-3 cells and PC-3 cells showed significant amounts of uptake of spherulites (Fig. 5a). The nonspecific interaction was significantly inhibited following the incorporation of 3 mol% of PEG_{2k}- or PEG_{5k}-conjugate (Fig. 5b, c) with PEG_{5k} being more effective in providing the shielding effects. Replacement of the non-targeting PEG-lipid with SV119-ligand-modified $PEG_{3.5k}$-DOA led to the restoration of cellular uptake to a level that was similar to that of unmodified spherulites, suggesting that the effective uptake of SV-119-targeted spherulites by PC-3 tumor cells was mediated by the specific ligand introduced.

It should be noted that despite the clear demonstration of the shielding/stabilizing effect of post-inserted PEG-DOA and the targeting capability of the post-inserted SV-119-PEG-DOA, the formulations reported here are far from being optimized. We also did not quantitatively measure the amounts of PEG conjugates incorporated into the spherulites considering the high efficiency of postinsertion approach with both unilamellar liposomes and spherulites (23, 25). More studies are needed in the future to define the optimal amounts of PEG-lipid and ligand-derivatized PEG-lipid for *in vivo* drug delivery.

Effect of Dexamethasone on Loading Efficiency and Release Profile of Spherulites

Our results, as well as others' clearly showed that CH plays a crucial role in the improvement of the membrane stability and drug retention. Dexamethasone (Dex), a more water soluble steroid anti-inflammatory drug that shares some structural similarity with CH (Fig. 6) was investigated as a co-lipid in spherulites in place of CH. Formulations **8–10** (Table 3) with gradually increased Dex to CH ratios were prepared and examined for drug retention and cargo release kinetics over

Table 3 Formulation Composition, Particle Sizes and Entrapment Efficiency of Spherulites with Varied Amounts of Dexamethasone and Cholesterol

Formulation (m/m)		Particle size (nm)	EE (%)
#	SPC/BS10/CH/Dex		
4	57/14/29/0	275.00±8.54	54.96±3.52
8	57/14/21/8	318.05±15.15	65.74±1.02
9	57/14/14/15	332.55±24.75	66.19±3.90
10	57/14/0/29	276.10±1.10	64.07±2.88

time in buffer at 37°C. It is apparent that increases in amounts of Dex led to a gradual increase in the rate of calcein release (Fig. 4c), suggesting that Dex is relatively weak in maintaining the stability of the lipid membrane. Interestingly, Dex-containing formulations gave higher calcein entrapment efficiency. Incorporation of as low as 8 mol% of Dex in spherulites led to a nearly 10% increase in EE for calcein (Table 3). The mechanisms for the increased EE for Dex-containing formulations are not clear. It is possible that the higher hydrophilicity of Dex may improve membrane hydration, leading to an increased EE. Alternatively, possible interaction between Dex and calcein may also play a role that contributes to the increased EE. More study on structure-activity relationship (SAR) of cholesterol and its derivatives may lead to the development of new liposomal formulations with improved EE and stability.

CONCLUSION

We have shown that both small and macromolecules can be effectively loaded onto spherulites. Our results showed that lipid ingredients employed in the formulation, especially the choice of surfactant and the amount of cholesterol play an important role in the biophysical properties of the spherulites including sizes, EE and release profiles. The spherulites can be further rendered serum-resistant *via* PEGylation. More importantly, incorporation of SV-119, a small molecule ligand for σ2 receptor led to a selective delivery of rhodamine-labeled spherulites to tumor cells that overexpress this receptor. Our formulations may represent a platform for selective delivery of various types of hydrophilic as well as hydrophobic therapeutics to target cells.

ACKNOWLEDGMENTS AND DISCLOSURES

This work was supported in part by NIH grants R01HL091828, R21CA128415 and R21CA155983.

REFERENCES

1. Torchilin VP. Multifunctional nanocarriers. Adv Drug Deliv Rev. 2006;58(14):1532–55.
2. Moghimi SM, Hunter AC, Murray JC. Long-circulating and target-specific nanoparticles: theory to practice. Pharmacol Rev. 2001;53(2):283–318.
3. Torchilin VP. Micellar nanocarriers: pharmaceutical perspectives. Pharm Res. 2007;24(1):1–16.
4. Sutton D, Nasongkla N, Blanco E, Gao J. Functionalized micellar systems for cancer targeted drug delivery. Pharm Res. 2007;24(6):1029–46.
5. Forrest ML, Yáñez JA, Remsberg CM, Ohgami Y, Kwon GS, Davies NM. Paclitaxel prodrugs with sustained release and high solubility in poly(ethylene glycol)-b-poly(e-caprolactone) micelle nanocarriers: pharmacokinetic disposition, tolerability, and cytotoxicity. Pharm Res. 2008;25(1):194–206.
6. Fonseca MJ, Jagtenberg JC, Haisma HJ, Storm G. Liposome-mediated targeting of enzymes to cancer cells for site-specific activation of prodrugs: comparison with the corresponding antibody–enzyme conjugate. Pharm Res. 2003;20(3):423–8.
7. Bangham AD, Horne RW. Negative staining of phospholipids and their structural modification by surface-active agents as observed in the electron microscope. J Mol Biol. 1964;8(5):660–8.
8. Samad A, Sultana Y, Aqil M. Liposomal drug delivery systems: an update review. Curr Drug Deliv. 2007;4(4):297–305.
9. Abu Lila AS, Ishida T, Kiwada H. Targeting anticancer drugs to tumor vasculature using cationic liposomes. Pharm Res. 2010;27(7):1171–83.
10. Lian T, Ho RJY. Trends and developments in liposome drug delivery systems. J Pharm Sci. 2001;90(6):667–80.
11. Torchilin V. Tumor delivery of macromolecular drugs based on the EPR effect. Adv Drug Deliv Rev. 2011;63(3):131–5.
12. Maeda H, Wu J, Sawa T, Matsumura Y, Hori K. Tumor vascular permeability and the EPR effect in macromolecular therapeutics: a review. J Control Release. 2000;65(1–2):271–84.
13. Xiang G, Wu J, Lu Y, Liu Z, Lee RJ. Synthesis and evaluation of a novel ligand for folate-mediated targeting liposomes. Int J Pharm. 2008;356(1–2):29–36.
14. Gantert M, Lewrick F, Adrian JE, Rössler J, Steenpaß T, Schubert R, *et al.* Receptor-specific targeting with liposomes *in vitro* based on sterol-PEG1300 anchors. Pharm Res. 2009;26(3):529–38.
15. Haran G, Cohen R, Bar LK, Barenholz Y. Transmembrane ammonium sulfate gradients in liposomes produce efficient and stable entrapment of amphipathic weak bases. Biochim Biophys Acta. 1993;1151(2):201–15.
16. Diat O, Roux D, Nallet F. Effect of shear on a lyotropic lamellar phase. J Phys II France. 1993;3(9):1427–52.
17. Diat O, Roux D. Preparation of monodisperse multilayer vesicles of controlled size and high encapsulation ratio. J Phys II France. 1993;3(1):9–14.
18. Redkar M, Hassan PA, Aswal V, Devarajan P. Onion phases of PEG-8 distearate. J Pharm Sci. 2007;96(9):2436–45.
19. Gauffre F, Roux D. Studying a new type of surfactant aggregate ("spherulites") as chemical microreactors. A first example: copper ion entrapping and particle synthesis. Langmuir. 1999;15(11):3738–47.
20. Mignet N, Brun A, Degert C, Delord B, Roux D, Helene C, *et al.* The spherulites™: a promising carrier for oligonucleotide delivery. Nucleic Acids Res. 2000;28(16):3134–42.
21. Zhang Y, Huang Y, Zhang P, Gao X, Gibbs RB, Li S. Incorporation of a selective σ-2 receptor ligand enhances uptake of liposomes by multiple cancer cells. Int J Nanomedicine. 2012;7:4473–85.
22. Zhang P, Ye H, Min T, Zhang C. Water soluble poly(ethylene glycol) prodrug of silybin: design, synthesis, and characterization. J Appl Polym Sci. 2008;107(5):3230–5.
23. Uster PS, Allen TM, Danie BE, Mendez CJ, Newman MS, Zhu GZ. Insertion of poly(ethylene glycol) derivatized phospholipid into pre-formed liposomes results in prolonged *in vivo* circulation time. FEBS Lett. 1996;386(2–3):243–6.
24. Szoka F. Comparative properties and methods of preparation of lipid vesicles (liposomes). Ann Rev Biophys Bioeng. 1980;9:467–508.
25. Simard P, Hoarau D, Khalid MN, Roux E, Leroux J-C. Preparation and *in vivo* evaluation of PEGylated spherulite formulations. Biochim Biophys Acta. 2005;1715(1):37–48.
26. Sułkowski WW, Pentak D, Nowak K, Sułkowska A. The influence of temperature, cholesterol content and pH on liposome stability. J Mol Struct. 2005;744:737–47.
27. Demel RA, Kinsky SC, Kinsky CB, van Deesen LLM. Effects of temperature and cholesterol on the glucose permeability of liposomes

prepared with neutral and synthetic lecithins. Biochim Biophys Acta. 1968;150(4):655–65.
28. Demel RA, De Kruyff B. The function of sterols in membranes. Biochim Biophys Acta. 1976;457(2):109–32.
29. Kim JC, Kim JD. Release property of temperature-sensitive liposome containing poly(N-isopropylacrylamide). Colloids Surf B. 2002;24(1):45–52.
30. Mu X, Zhong Z. Preparation and properties of poly(vinyl alcohol)-stabilized liposomes. Int J Pharm. 2006;318(1–2):55–61.
31. Senior JH. Fate and behaviour of liposomes *in vivo*: a review of controlling factors. Crit Rev Ther Drug Carrier Syst. 1987;3(2):123–93.
32. Semple SC, Chonn A, Cullis PR. Interactions of liposomes and lipid-based carrier systems with blood proteins: relation to clearance behaviour *in vivo*. Adv Drug Deliv Rev. 1998;32(1–2):3–17.
33. Nikolova AN, Jones MN. Effect of grafted PEG-2000 on the size and permeability of vesicles. Biochim Biophys Acta. 1996;1304(2):120–8.
34. Chonn A, Cullis PR. Ganglioside GM1 and hydrophilic polymers increase liposome circulation times by inhibiting the association of blood proteins. J Liposome Res. 1992;2(3):397–410.
35. Blume G, Cevc G. Liposomes for the sustained drug release *in vivo*. Biochim Biophys Acta. 1990;1029(1):91–7.
36. Vilner BJ, John CS, Bowen WD. Sigma-1 and sigma-2 receptors are expressed in a wide variety of human and rodent tumor-cell lines. Cancer Res. 1995;55(2):408–13.
37. Wheeler KT, Wang LM, Wallen CA, Childers SR, Cline JM, Keng PC, *et al*. Sigma-2 receptors as a biomarker of proliferation in solid tumours. Br J Cancer. 2000;82(6):1223–32.
38. Mach RH, Smith CR, AlNabulsi I, Whirrett BR, Childers SR, Wheeler KT. Sigma-2 receptors as potential biomarkers of proliferation in breast cancer. Cancer Res. 1997;57(1):156–61.
39. Colabufo NA, Berardi F, Contino M, Ferorelli S, Niso M, Perrone R, *et al*. Correlation between sigma2 receptor protein expression and histopathologic grade in human bladder cancer. Cancer Lett. 2006;237(1):83–8.
40. Kashiwagi H, McDunn JE, Simon PO, Goedegebuure PS, Xu J, Jones L, *et al*. Selective sigma-2 ligands preferentially bind to pancreatic adenocarcinomas: applications in diagnostic imaging and therapy. Mol Cancer. 2007;6(48):48–59.
41. Spitzer D, Simon Jr PO, Kashiwagi H, Xu J, Zeng C, Vangveravong S, *et al*. Use of multifunctional sigma-2 receptor ligand conjugates to trigger cancer-selective cell death signaling. Cancer Res. 2012;72(1):201–9.
42. Wang Y, Xu J, Xia X, Yang M, Vangveravong S, Chen J, *et al*. SV119-gold nanocage conjugates: a new platform for targeting cancer cells *via* sigma-2 receptors. Nanoscale. 2012;4(2):421–4.